MINISTRY OF EDUCATION AND TRAINING
UNIVERSITY OF TRANSPORT AND COMMUNICATIONS

NGUYEN HAI HA

STUDY ON THE BEHAVIOR OF STONE COLUMNS COMBINED WITH GEOGRID REINFORCEMENT FOR SOFT SOIL TREATMENT IN TRANSPORTATION INFRASTRUCTURE CONSTRUCTION

Major: Transportation Construction Engineering
Code: 9580205

SUMMARY OF DOCTORAL DISSERTATION

HANOI – 2026

This dissertation was completed at:
University of Transport and Communications

Supervisors:

1. **Assoc. Prof. Dr. Nguyen Duc Manh**
   University of Transport and Communications
2. **Assoc. Prof. Dr. Dang Hong Lam**
   University of Transport and Communications

Reviewer 1:

Reviewer 2:

Reviewer 3:

This dissertation will be defended before the University-level Dissertation Evaluation Committee at the University of Transport and Communications at … o'clock on … / … / …..

The dissertation can be found at the following libraries:
Vietnam National Library
Library of the University of Transport and Communications

INTRODUCTION

1. Rationale of the study

Vietnam's transportation infrastructure system is receiving very large investment, especially the expressway and high-speed railway networks. The widespread presence of soft soil layers in the Red River Delta, the central coastal region, and the Mekong Delta poses significant challenges for transportation infrastructure construction, particularly where the soft soil thickness exceeds (15–20) m.

In addition to conventional measures (preloading, prefabricated vertical drains, sand compaction piles, soil-cement columns, reinforced concrete piles), the stone column (SC) solution - commonly crushed-stone columns - combined with a geogrid (GG) layer spread over the column heads has been increasingly studied and widely applied worldwide. This column-geogrid system belongs to the group of Geosynthetic-Reinforced Column-Supported (GRCS) embankment solutions, in which the stone column acts as the main load-bearing element, while the geogrid layer spread over the column heads forms a load-transfer platform that distributes the load from the embankment to the columns and the surrounding soft ground.

The working mechanism of the GRCS system relies on the combination of the soil arching effect formed within the embankment above the load-transfer platform, which concentrates load onto the column heads, and the membrane effect of the geogrid layer, which allows additional load from the soil between columns to be transferred to the column heads through tension in the geogrid. This solution offers several advantages: effective treatment of thick soft soil deposits, fast construction, lower cost compared with rigid piles, and reduced total and differential settlement at the embankment surface.

The stone-column-geogrid embankment solution has been successfully applied in several countries: the Berlin–Hamburg railway line (Germany), the M60 motorway (United Kingdom), and road–rail projects in Japan. Design standards such as EBGEO (Germany), BS 8006 (United Kingdom), and FHWA (United States) provide fairly detailed guidance for the design calculation of GRCS systems.

In Vietnam, stone columns have been applied in a number of soft soil treatment projects, but the combination of stone columns with a geogrid layer into a complete system remains little studied, and no design calculation guidance suitable for Vietnamese conditions is yet available. Several issues remain unresolved: theoretically, existing methods for the soil arching effect give results differing by (20–40)%; the determination of the stress concentration ratio for stone columns remains debated owing to deformation characteristics different from those of rigid piles. Experimentally, systematic data under Vietnamese conditions are lacking. In terms of application, no suitable design calculation procedure yet exists.

Based on the above analysis, the dissertation "Study on the behavior of stone columns combined with geogrid reinforcement for soft soil treatment in transportation infrastructure construction" was carried out to clarify the working mechanism of the soil–stone column–geogrid system, to evaluate the influence of key factors on load-transfer efficiency, to propose more suitable calibrated calculation formulas, and to provide a scientific basis for applying this solution in Vietnam.

2. Research objectives

- To clarify the working mechanism and behavior of the stone-column-geogrid system under embankment loading, considering the soil arching effect, the behavior of the geogrid within the load-transfer platform, the stress distribution between the columns and the surrounding ground, and the load–settlement relationship of the system.

- To evaluate the influence of key factors on working efficiency, including material properties (column material, foundation soil, geogrid), column arrangement (single column/group of columns, spacing ratio s/D), load-transfer platform configuration, and embankment height.

- To propose suitable calculation formulas for determining the stress concentration ratio (SCR) and the bearing capacity (BC) of the stone-column-geogrid system, verified against experimental results and numerical simulation, to support the design of soft soil treatment for transportation infrastructure construction in Vietnam.

3. Research subject and scope

Research subject: The soft soil- stone column- geogrid system under embankment loading in transportation infrastructure construction. The geogrid layer spread over the column heads acts as the load-transfer platform from the embankment.

Research scope:

- Methodologically: combining reduced-scale (1:20) physical model (PM) tests in the laboratory with three-dimensional numerical model (NM) analysis using the Plaxis 3D finite-element software.

- Test conditions: ordinary single stone columns and single stone columns combined with a geogrid layer in clayey silt at three consistency states (I_L = 0.78; 1.0; 1.5); stone column groups (2×2 arrangement) combined with a geogrid layer in clayey silt at the soft-plastic state (I_L = 0.78) with three spacing ratios s/D = 2.5; 3.0; 3.5. Column material: crushed stone. Loading: static vertical loading.

- The dissertation does not consider the effects of lateral loading, dynamic loading, multi-layered geological structure, negative skin friction, overall embankment slope stability, time-dependent groundwater-level fluctuation, or the case of a stone column wrapped by a geogrid casing.

4. Scientific and practical significance

Scientific significance:

- Development of a systematic experimental dataset on the mechanical behavior (load–settlement–stress distribution–stress concentration ratio) of the stone-column-geogrid system under conditions representative of soft soil in Vietnam, using a 1:20-scale physical model.

- Clarification of the influence of the column spacing ratio (s/D), the physical state of the foundation soil (I_L), and the presence of the geogrid on the stress concentration ratio, the settlement reduction ratio, and the bearing capacity of the system.

- Proposal of calibrated formulas for predicting the ultimate bearing capacity, the stress concentration ratio (n), and the settlement reduction ratio (β) appropriate to the research subject and scope.

Practical significance:

- Provision of a scientific basis and empirical data for applying the stone-column-geogrid solution in Vietnam, particularly in the construction of road embankments on soft soil.

- The research results can support additions to current soft soil design standards and serve as reference material for teaching and training in the field of geotechnical engineering.

5. Dissertation structure

In addition to the introduction and conclusions, the dissertation comprises four chapters:

- Chapter 1: Overview of research on stone columns combined with geogrid reinforcement in soft soil treatment.

- Chapter 2: Theoretical basis for calculation and modeling of the stone-column-geogrid system.

- Chapter 3: Experimental study of stone columns combined with geogrid reinforcement on a laboratory physical model.

- Chapter 4: Behavior of stone columns combined with geogrid reinforcement in soft soil treatment under embankment loading.

CHAPTER 1
OVERVIEW OF RESEARCH ON STONE COLUMNS COMBINED WITH GEOGRID REINFORCEMENT IN SOFT SOIL TREATMENT

1.1. Overview of soft soil in transportation infrastructure

1.1.1. Soft soil and classification of soft soil

Soft ground characterized by low undrained shear strength (c_u < 25 kPa), small deformation modulus (E < 10 MPa) and high compressibility has always been a challenge in transportation infrastructure construction in Vietnam. Saturated soft clay, clayey mud and peat layers are widely distributed in the Mekong Delta, the Red River Delta and the central coastal strip, typically with thicknesses from 10 m to over 30 m.

According to Terzaghi and Peck (1996), soft clay has S_u < 25 kPa and N_{SPT} < 4. Standard TCCS 41:2022/TCĐBVN specifies that very soft clay has e ≥ 1.5, soft silty clay has e ≥ 1.0; shear strength ≤ 15 kPa and internal friction angle φ_u < 10° or S_u ≤ 35 kPa. The liquidity index I_L is an important indicator: when $I_L \approx 1$, the soil transitions from the soft plastic to the liquid state; when $I_L > 1$, the soil is in a nearly liquid state.

Soft soil classification in transportation infrastructure construction can be approached from multiple angles: by grain-size composition and Atterberg limits (USCS system – ASTM D2487); by liquidity index I_L to assess the physical state; by origin (marine sediment, delta deposit, organic soil/peat) to predict long-term compression trends; and by combining mechanical indicators (S_u, N_{SPT}, E, C_c, k_v, OCR) to quantify risk and select an appropriate treatment solution.

1.1.2. Soft soil treatment solutions for large soft soil thickness

When the soft soil thickness exceeds about (10–15) m, simple measures such as soil replacement or preloading are generally no longer effective. Current design guidance groups treatment solutions by their main working mechanism into: (1) preloading combined with vertical drainage; (2) use of piles or columns to create a composite foundation; (3) load reduction and special embankment forms; and (4) in-situ soil stabilization.

Among these, embankments on piles/columns combined with a geosynthetic-reinforced load-transfer platform are becoming increasingly common. This system is divided into two main branches: the GRPS (Geosynthetic Reinforced Pile-Supported) embankment - on rigid piles reinforced with geogrid; and the GRCS (Geosynthetic Reinforced Column-Supported) embankment - on stone columns reinforced with geogrid. The two systems differ in load-bearing capacity and load distribution characteristics and need detailed study for appropriate design calculation.

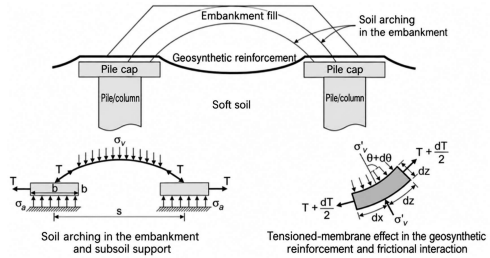

Figure 1.1 Load-transfer mechanism of an embankment on a geogrid-reinforced column system

1.1.3. Development trends and research orientation

Stone columns combined with geosynthetic reinforcement, including the geogrid-encased form (GESC) and the form with a geogrid layer spread horizontally over the column group heads (GRCS), are considered a solution with the potential to balance economic and technical factors, particularly for long road sections on thick, soft clay. According to EBGEO (2011), design should simultaneously consider three mechanisms: the arching effect within the embankment, the membrane effect of the geogrid reinforcement layer, and the bearing capacity of the soft soil zone between columns.

1.2. Overview of research on stone columns

1.2.1. Stone columns and their application in soft soil treatment

Within the scope of this dissertation, the term "stone column (SC)" is used consistently to refer to a stone column constructed by the deep vibro technique with crushed stone aggregate. The deformation modulus of stone columns is typically in the range of (25–40) MPa, reaching (30–70) MPa in some cases when the material is well compacted.

The main working mechanisms of stone columns include: (i) replacement of soft soil and stress concentration; (ii) reinforcement and restraint of lateral deformation; (iii) drainage and acceleration of consolidation. The main failure modes are:

bulging, punching shear, general shear failure and block failure. Hughes and Withers (1974) described the bulging zone as concentrated at a depth of about (2–4)D from the column head. McKelvey et al. (2004) confirmed that bulging occurs along the entire column length when L/D < 6, and only in the upper part when L/D > 10.

1.2.2. Stone column research worldwide and in Vietnam

Stone column technology originated in Europe, stemming from the deep vibro method developed by Keller in the 1930s in Germany. From the 1970s, Hughes and Withers (1974) proposed a formula for the ultimate bearing capacity; Barksdale and Bachus (1983) established a bearing capacity factor $N_c \approx 5$ and a stress concentration ratio of 2.5–5.0 for FHWA. Priebe (1995) proposed an improvement-factor method based on a unit cell. Balaam and Booker (1981, 1985) derived an analytical solution for the column–soil interaction problem. From 2000 onward, research has focused on 3D finite-element modeling and on combining stone columns with geosynthetic reinforcement.

Stone columns have been applied in several projects in Vietnam, such as the Nghi Son oil refinery (Thanh Hoa) and PTSC Vung Tau. However, domestic research has so far remained mostly at the level of theoretical overview or simple numerical analysis of plain stone columns, with no in-depth experimental study yet on the behavior of stone columns combined with geogrid reinforcement.

1.2.3. Research on geogrid-reinforced stone columns under embankments

The working mechanism of the GRCS system is governed by three main factors: the arching effect within the embankment and the bedding layer; the load bearing and deformation capacity of the stone column in soft soil; and the membrane mechanism that arises when the geogrid deflects between column heads. Standards such as BS 8006-1:2010 and EBGEO (2011) provide a calculation framework for embankments on geogrid-reinforced columns, mainly focusing on modeling the arching effect and tension in the geogrid. However, dedicated publications specifically on stone columns combined with geogrid reinforcement for road embankments remain scarce, especially in Vietnam.

1.3. Some remaining issues

From the literature review, the main remaining issues identified are:

- On classification and modeling: there is no clear framework distinguishing the roles of geogrid-encased stone columns (GESC) and stone columns combined with a geogrid layer spread over the column heads (GRCS).
- On arching and geogrid tension formulas: the formulas in BS 8006-1 and EBGEO were mainly developed for rigid piles assuming the column head as a rigid support, without considering the significant compression–lateral bulging deformation of stone columns.
- The stress concentration ratio varies considerably in soft soil rather than remaining constant as assumed by the standards; the range of variation is quite wide (from 1.5–6.0 according to McCabe et al., 2009).
- On the current status in Vietnam: there is no systematic experimental data on stone columns combined with geogrid reinforcement; no design calculation procedure suitable for domestic conditions is yet available.

1.4. Discussion and proposed research issues

Stone columns are a deep soft-soil treatment solution with many advantages: they act both as a load-bearing element and as a "vertical drainage well". Combining stone columns with a geogrid layer spread over the heads of a column group simultaneously exploits the arching effect and the tension membrane effect, optimizing load distribution, which is particularly suitable for wide-area embankments. However, most current design formulas (FHWA, BS 8006, EBGEO) were developed for rigid piles, and the behavior of the stone-column-geogrid system according to the state of the foundation soil has not been fully verified.

From the above analysis, four main research issues are identified:

(1) Experimental study on a physical model of single stone columns and stone column groups (2×2) combined with geogrid reinforcement in clay typical of the Red River Delta, at three physical states (I_L = 0.78; 1.0; 1.5) and varying column spacing (s/D = 2.5; 3.0; 3.5).

(2) Quantitative analysis of the influence of the main parameters (s/D, J, Ec, I_L) on treatment efficiency through the physical model and the numerical model.

(3) Development and verification of a 3D numerical model on the Plaxis platform, calibrated against experimental results, to extend the parametric study.

(4) Assessment of the suitability of current formulas and standards, and proposal of calibrations for design purposes.

1.5. Research approach and methodology

The dissertation adopts an integrated four-step approach: (1) systematizing theory → (2) experimental study on a 1:20-scale reduced physical model → (3) 3D numerical model analysis using Plaxis 3D → (4) synthesis, regression analysis and proposal of calculation formulas. The combination of the physical model and the numerical model forms the main methodological framework, in which the physical model provides empirical data to calibrate the numerical model, while the numerical model allows the parametric study to be extended and the results to be generalized.

CHAPTER 2
THEORETICAL BASIS FOR CALCULATION AND MODELING OF THE STONE-COLUMN-GEOGRID SYSTEM

Chapter 2 presents the systematic theoretical basis for the calculation and modeling of the stone-column-geogrid system (GRCS) in soft soil treatment under embankment loading, in which the stone column acts as the main load-bearing element while the geogrid spread over the column heads acts as the load-transfer platform. Three main load-transfer mechanisms operate simultaneously: the arching effect within the embankment, the membrane effect of the geogrid, and stress concentration due to the stiffness difference between the column and the foundation soil.

2.1. Stone column parameters and determination methods

The three most important parameters governing reinforcement efficiency are: the column deformation modulus E_c, the stress concentration ratio n, and the geogrid stiffness J.

Deformation modulus E_c: According to Barksdale and Bachus (1983), E_c = (30–58) MPa for stone columns; McCabe et al. (2009) extend this up to 70 MPa. With E_s of soft clay around (1.5–5) MPa, the actual E_c/E_s ratio is about 6–47. Unlike concrete, the stone column material exhibits clearly nonlinear behavior, with stiffness increasing as the confining pressure increases, described by a power-law relationship:

$$E_c = E_{ref}\left(\frac{\sigma_3'}{p_{ref}}\right)^m \quad (2\text{-}1)$$

where: E_{ref}: reference deformation modulus, from (30–50) MPa for compacted crushed stone; pref: reference pressure (usually 100 kPa); σ'_3: effective lateral pressure; m: exponent (m ≈ 0.5 for granular material per Janbu, 1963).

Stress concentration ratio n: Defined as the ratio between the stress on the column head σc and the stress on the foundation soil σs: $n = \sigma_c / \sigma_s$. The coefficient n is not a constant but a variable depending on time and the working stage. During immediate loading, n is usually low (n = 2–3); during the stable stage after consolidation, n can reach 4 to 6 or higher. According to FHWA (1983), there is a linear relationship between n and the stiffness ratio: $n = \alpha\cdot(E_c/E_s)$ with α = 0.2–0.4. With a geogrid present, n is always greater than for the unreinforced system due to the membrane effect, and is a function n = f(J, δ, E_c, E_s).

Geogrid stiffness J: Determined from the slope of the tensile force–strain curve: J = T/ε (kN/m). The reinforcing effect increases strongly as J increases from 0 to 2000 kN/m; when J > 4000 kN/m, the additional improvement becomes negligible.

2.2. Ultimate bearing capacity theory for stone columns

2.2.1. Single stone column

According to the cylindrical cavity expansion theory (Hughes and Withers, 1974), the ultimate bearing capacity q_{ult} of a single column is mainly governed by bulging failure:

$$q_{ult} = \sigma_{rL}\cdot K_p = \sigma_{rL}\cdot \tan^2(45° + \varphi_c/2) \quad (2\text{-}2)$$

where: Kp: passive earth pressure coefficient; φc: internal friction angle of the column material; σ_{rL}: ultimate lateral pressure of the foundation soil. The ultimate lateral pressure σ_{rL} is determined according to elastic–plastic theory (Gibson and Anderson, 1961):

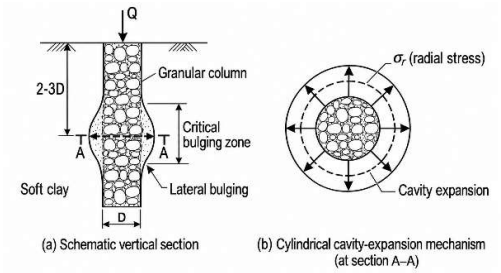

Figure 2.1 Bulging failure mechanism of a single stone column in soft clay

$$\sigma_{rL} = \sigma_{ro} + c_u\cdot[1 + \ln(E_s/(2\cdot(1+\nu)\cdot c_u))] \quad (2\text{-}3)$$

The bulging zone is concentrated within (1–2)D, with a maximum depth of up to 4D. FHWA (1983) proposes a simplified formula: $q_{ult} = N_c\cdot c_u$ with $N_c \approx 5$.

2.2.2. Stone column groups

For column groups without geogrid, the Priebe (1995) method is based on a unit cell with the following stress equilibrium equation:

$$\sigma = \sigma_c\cdot a_s + \sigma_s\cdot(1 - a_s) \quad (2\text{-}4)$$

where: as: area replacement ratio.

When a geogrid is placed over the column heads, two additional mechanisms appear: the membrane effect and the confinement effect. The deflected geogrid develops a tensile force T, reducing the pressure on the soft soil and transferring load toward the column heads.

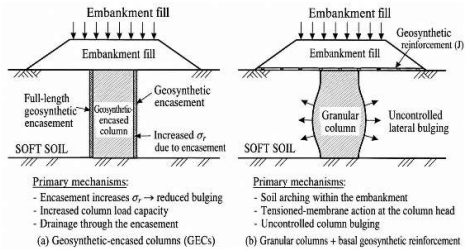

Figure 2.2 Working mechanisms of the geogrid over the column heads

The vertical force equilibrium equation on a geogrid element is:

$$2T\sin\theta = (p_s - p_p).(s - D) \quad (2\text{-}5)$$

where: T: tensile force in the geogrid; θ: rotation angle at the column edge; ps: vertical stress beneath the geogrid; pp: stress on the column head; s: column center-to-center spacing; D: column diameter.

2.3. Settlement prediction for stone columns in soft soil treatment

2.3.1. The Priebe (1995) improvement-factor method

The settlement of the improved ground St is computed from the settlement of the untreated ground So via the basic improvement factor n_0: St = So / n_0

With a Poisson's ratio ν = 1/3, n_0 is determined as a function of the area replacement ratio as and the active earth pressure coefficient K_a of the column material.

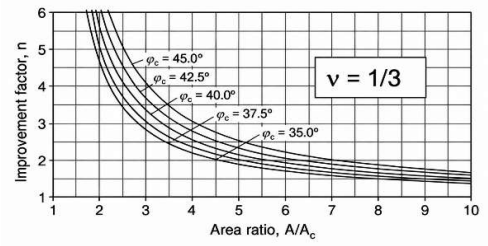

Figure 2.3 Relationship between the area ratio and the basic improvement factor

Limitation: the assumption of uniform bulging along the full column length does not match reality (the bulging zone is actually concentrated at 2–4D).

2.3.2. The Aboshi (1979) and Balaam–Booker (1981, 1985) methods

Aboshi et al. (1979) proposed a settlement reduction ratio based on a unit cell and one-dimensional consolidation: $S/S0 = 1/[1 + as\cdot(n - 1)]$. FHWA (1983) recommends n = 3–5.

Balaam and Booker (1981, 1985) developed an analytical solution based on cavity expansion theory combined with the unit-cell concept and an axisymmetric elastic–plastic finite-element analysis: St = β · S0 with β = f(ν, Ac/A). The 1985 version added Mohr-Coulomb plastic yielding with a non-associated flow rule. Law (2015) compared this with Plaxis 3D results and showed that the Balaam–Booker (1981) method overestimates the improvement factor due to the linear-elastic

assumption.

2.3.3. Effect of the geogrid on settlement

With a geogrid in place, the total settlement, and especially the differential settlement between the column and the surrounding soil, is significantly reduced. The geogrid helps to equalize settlement; an increase in the stress concentration ratio n means the column carries more load, reducing the compressive stress on the soft soil.

2.4. Theory of the behavior of the embankment–stone column–geogrid system

2.4.1. Arching effect within the embankment

Arching forms when the soft soil between columns consolidates and settles while the column heads maintain their original position. Conditions for formation: a sufficiently large stiffness difference between the columns and the foundation soil; a sufficiently large embankment height H; and embankment fill material with internal frictional properties.

Figure 2.4 Mechanism of arching effect formation within the embankment

The main theoretical models include: (1) Hewlett and Randolph (1988), 3D hemispherical arching, Mohr-Coulomb limit equilibrium; (2) Low et al. (1994), 2D cylindrical arching (Terzaghi); (3) EBGEO (2011), 3D multi-layer arching following Zaeske (2001); (4) BS 8006-1:2010, the semi-empirical Marston method when $H < 1.4(s - a)$ and the Hewlett–Randolph method when $H \geq 1.4(s - a)$.

Two quantities assess the degree of load transfer: the load-transfer efficiency $Ef = Pc/(\gamma H \cdot s^2)$ and the stress-reduction ratio $\rho = \sigma s/(\gamma H + q)$, related by: $Ef = 1 - \rho \cdot (1 - as)$.

2.4.2. Membrane effect of the geogrid

The membrane effect is activated when a differential settlement ΔS appears between the foundation soil and the column heads. The geogrid deforms into a sagging shape, generating a tensile force T with an upward-directed vertical component.

The analytical models include: (1) the deflected-membrane model (BS 8006-1:2010), with the geogrid under a uniformly distributed load and a parabolic deflection shape; (2) the tensioned-membrane model (Jones et al., 1990), with a nonlinear relationship $T = J \cdot \varepsilon$, considering the interaction with the subgrade through the subgrade reaction modulus k_s; (3) the combined arching–membrane model (Van Eekelen et al., 2013), analyzing both effects simultaneously on a concentric-arch model.

$$T_{rp} = W_T \cdot (s - a) / (2 \cdot a) \cdot (1/(1 + 1/(6\varepsilon)))^{0.5} \quad (2\text{-}6)$$

Theo EBGEO (2011): $$E_d = \sigma_{z,k} \cdot A_L / (2 \cdot (J \cdot \varepsilon_{max})^{0.5}) \quad (2\text{-}7)$$

2.4.3. Soil–column–geogrid interaction mechanism

The total load from the embankment is divided into the portion transferred to the column heads through the arching effect; the portion transferred through the geogrid via the membrane effect; and the portion acting directly on the soft foundation soil. Behavior analysis by stage: (i) construction stage, n reaches only 2–3; (ii) consolidation stage, n increases to 4–6; (iii) stable stage, n ranges from 4–8, lower than for reinforced-concrete rigid piles (n = 10–20).

2.4.4. Standard-based design methods

EBGEO (2011): applies the Zaeske multi-layer arching model, distinguishing between complete arching ($H \geq h_{cr}$) and incomplete arching, and considers the subgrade reaction in computing the geogrid tensile force. BS 8006-1:2010: computes the tensile force assuming the geogrid carries the entire load from the soil zone between columns (without considering the subgrade reaction). The BS 8006-1:2016 version added the Van Eekelen (2013) method.

2.5. Physical model theory and scaling

2.5.1. Types of physical models

The physical model (PM) is an indispensable tool in geotechnical engineering, comprising: the 1g model, the centrifuge model (N×g), and the full-scale (1:1) model.

Table 2.1 Comparison of the 1g model and the centrifuge model

Criterion	1g model	Centrifuge model
Gravitational acceleration	1 g (natural)	N (20–200)g
Scale ratio	1:10 – 1:50	1:50 – 1:200
Simulation of in-situ stress	Approximate, less accurate at large depth	Close approximation of the prototype stress field
Equipment cost	Low - moderate	Very high
Preparation time	Short (weeks)	Long (months)
Observation capability	Good (direct view, through glass, camera)	Limited, depends on the rotation and imaging system
Number of scenarios required	Large (10–20 scenarios)	Few (typically 3–5 scenarios)
Typical problems	Shallow foundations, small columngroups, embankments	Dams, deep tunnels, thick foundations, seismic problems

2.5.2. Model similitude and scaling

Model similitude is established based on dimensional analysis (Buckingham, 1914) and must simultaneously satisfy three types of similarity: geometric similarity ($\lambda_L = L_m/L_p$), kinematic similarity, and dynamic similarity. For the 1g model, the stress scale factor $\lambda_\sigma \approx 1$ in the zone of interest, accepting some error in the low-stress region. Boundary conditions: $D/d_{50} > 50$ (Muir Wood, 2004) or $D/d50 \geq 20$ (Murugesan and Rajagopal, 2010).

2.6. Chapter 2 remarks

Chapter 2 presented a systematic theoretical basis comprising: (i) three core parameters (E_c, n, J) and their determination methods; (ii) ultimate bearing capacity theory for single columns and column groups; (iii) settlement prediction methods (Priebe, Aboshi, Balaam–Booker); (iv) arching theory (Hewlett–Randolph, EBGEO, BS 8006) and membrane effect theory (deflected-membrane model, tensioned-membrane model, combined Van Eekelen model); (v) design methods according to the international standards EBGEO (2011) and BS 8006-1:2010; (vi) physical model theory and similitude laws.

Most current calculation methods were developed for reinforced-concrete rigid piles and do not fully reflect the behavior of stone columns, which have lower

stiffness, especially when combined with geogrid reinforcement in soft soil treatment. This gap needs to be addressed through physical-model testing combined with numerical modeling to verify and calibrate the theory and to propose calculation methods suitable for Vietnamese conditions - this is the content of Chapters 3 and 4.

CHAPTER 3
EXPERIMENTAL STUDY OF STONE COLUMNS COMBINED WITH GEOGRID REINFORCEMENT ON A LABORATORY PHYSICAL MODEL

Chapter 3 presents the construction and execution of reduced-scale physical model tests to investigate the behavior of the stone-column-geogrid system in soft soil under embankment loading. The analysis results provide a reference dataset for calibrating and verifying the 3D numerical model presented in Chapter 4.

3.1. Construction of the laboratory physical model

3.1.1. Selection of the research model

The 1g model was selected because it suits the research objective (investigating the column–geogrid–soil interaction mechanism, which mainly depends on ratios of mechanical and geometric quantities), suits the laboratory equipment conditions, has broad reference support from international studies (Hu, 1995; McKelvey et al., 2004; Black et al., 2011), and allows verification against a numerical model.

3.1.2. Selection of the 1:20 physical model scale

Three scale options - 1:15, 1:20 and 1:25 - were proposed for comparison. With an aggregate particle size $d_{50} \approx 2$ mm, the D/d_{50} ratios are 26.5, 20.0 and 16.0 respectively. The 1:20 scale was selected because: $D/d_{50} = 20.0$ exactly equals the minimum value recommended by Murugesan and Rajagopal (2010); the 1000×500×1000 mm tank dimensions satisfy the boundary conditions (distance from the edge column to the wall 6.25D > 5D, soil thickness below the column tip 6.7D > 3D); and it suits a group of 4 columns (2×2) with s/D = 2.5 to 3.5.

The principle of partial similitude was applied: (i) geometric parameters scaled down by n = 20; (ii) the load kept at the prototype stress level ($q = \gamma_{embankment} \times H_{embankment} + q_{traffic} = 18 \times 6 + 12 = 120$ kPa); (iii) foundation soil properties kept unchanged (c_u, φ, E_s); (iv) the geogrid kept as the control variable ($T^* = 200$ kN/m).

Table 3.1 Comparison of reduced-scale physical model options

Criterion	Scale 1:15	Scale 1:20	Scale 1:25
Column diameter D (mm)	53	40	32
Column length L (mm)	800	600	480
Ratio D/d50 (d50 = 2 mm)	26.5	20.0	16.0
Assessment D/d50 ≥ 20	Good	Satisfactory	Not satisfactory
Minimum tank size (mm)	1330×665×1200	1000×500×1000	800×400×800
Tank volume (m³)	1.06	0.50	0.26
Estimated soft soil mass (kg)	~1600	~750	~390
Expected model error (%)	5-8	8-12	15-20
Feasibility of laboratory setup	Difficult	Suitable	Favorable
Overall assessment	Good, bulky	**Optimal balance**	Reduced accuracy

The validity of the 1:20 scale was verified by numerical simulation in Plaxis 3D: a comparison between the 1:1 prototype model and the 1:20 reduced-scale model showed that the similitude theory is well satisfied in terms of stress distribution, settlement, and column-group effects.

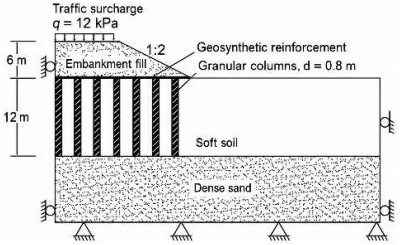

Figure 3.1 Physical setup of the stone-column-geogrid system

Table 3.2 Scaling of parameters from the prototype to the 1:20-scale model

Parameter	Symbol	Prototype	PM (1:20)	Scaling principle	Unit
Soft soil thickness	$H_{softsoil}$	12.000	600	Geometric (÷n)	mm
Embankment fill height	$H_{embankment}$	6.000	300	Geometric (÷n)	mm
Column diameter	D	800	40	Geometric (÷n)	mm
Column length	L	12.000	600	Geometric (÷n)	mm
Foundation soil properties	c_u, φ, E_s	Unchanged	Unchanged	Failure criterion preserved	-
Geogrid stiffness	J	2.000	2.000	Control variable (unchanged)	kN/m
Geogrid tensile strength	T	200	200	Control variable (unchanged)	kN/m
Distributed load	q*	-	120	Stress level preserved	kPa

3.1.3. Model setup and test apparatus

Test materials:

- Soft soil: clayey silt taken at a depth of 3 m in Thuong Tin, Hanoi, in the soft-plastic state ($I_L = 0.78$), representative soft soil of the Thai Binh Formation in the Red River Delta. For the single-column tests, soil was additionally prepared at $I_L = 1.0$ and $I_L = 1.5$.

Table 3.3 Basic physical properties of the soft soil used in the study

Property	Symbol	Unit	Value
Natural moisture content	W	%	46.8
Liquid limit	W_L	%	50.1
Plastic limit	W_P	%	35.4
Plasticity index	I_P	%	14.7
Liquidity index	I_L	-	0.78
Unit weight	γ	kN/m³	16.6
Initial void ratio	e_o	-	1.313
Grain-size composition:			
particle size <0.005 mm	-	%	26.1
particle size (0.005 – 0.05) mm	-	%	49.9
particle size > 0.05 mm	-	%	24

- Stone column aggregate: crushed stone, gradation 0.5–4.75 mm scaled down from the 20–75 mm gradation, $d_{50} = 1.83$ mm, friction angle $\varphi_c = 38° \pm 2°$, $\rho_s = 2.65$ g/cm³,

relative density ID = 0.96.

Table 3.4 Physical properties of the aggregate used for the stone columns

No.	Criterion	Symbol	Unit	Value	Standard
1	Specific gravity	ρ_s	g/cm³	2.65	TCVN 7572-4
2	Minimum (loose) bulk density	$\rho_{d,min}$	g/cm³	1.42	TCVN 7572-6
3	Maximum (dense) bulk density	$\rho_{d,max}$	g/cm³	1.68	TCVN 7572-6
4	Internal friction angle	φ	degree	38± 2	Large direct shear
5	Los Angeles abrasion	LA	%	22	TCVN 7572-12

– Geogrid: nominal tensile strength 200 kN/m (machine direction: 209.4 kN/m; cross direction: 105.7 kN/m), tensile modulus at ε = 2%: J = 2070 kN/m.

Table 3.5 Technical specifications of the geogrid

No.	Parameter	Equipment	Unit	Value
1	Tensile strength at break, machine direction	X500-100	kN/m	209.4
2	Elongation at break, machine direction	X500-100	%	12
3	Tensile strength at 2% elongation, machine direction	X500-100	kN/m	41.4
4	Tensile strength at 5% elongation, machine direction	X500-100	kN/m	78.7
5	Tensile strength at break, cross direction	X500-100	kN/m	105.7
6	Tensile modulus at 2% elongation	-	kN/m	2070

Loading and measurement system: a steel loading frame rated at 50 kN; a load ring with 0.01 mm graduations; LVDT sensors to measure settlement; strain gauges to measure geogrid strain and column-head stress; load cells to measure soil pressure; a Data Logger for automatic data acquisition.

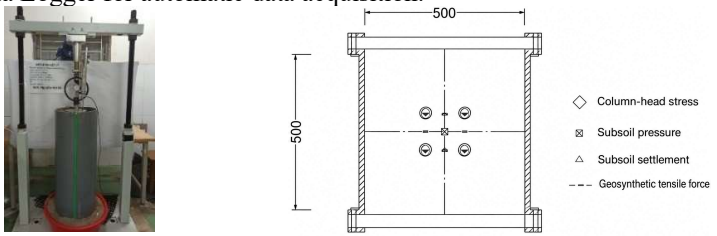

Figure 3.2 Loading frame and layout of the instrumentation system in the physical model

3.1.4. Model quality control

Quality control ensured three principles: consistency, repeatability and traceability. The soft soil was controlled through the moisture–shear-strength correlation using a Swedish fall-cone penetrometer. The column aggregate was controlled to ID ≥ 0.95. The repeat-test error was < 5%, lower than the 10% criterion of Garnier et al. (2007).

Table 3.6 Summary of basic soil properties used in the physical model

No.	Criterion	Symbol	Unit	Liquidity index			Tolerance
				0.78	1.0	1.5	
1	Moisture content	W	%	46.7	50.1	57.8	±2%
2	Undrained shear strength	c_u	kPa	20	10	5	±10%
3	Deformation modulus	E_s	kPa	1450	1050	850	±15%
4	Physical state	-	-	Soft-plastic	Liquid	Liquid	3.2. Experimental study on the physical model

3.2.1. Test matrix and loading procedure

A total of 9 scenarios, each repeated twice (18 tests): 6 single-column tests (3 physical states × 2 types, with/without geogrid) and 3 column-group tests (2×2) at 3 spacing ratios s/D = 2.5; 3.0; 3.5). The Constant Rate of Penetration (CRP) method was used at a rate of 0.061 mm/min, with each load held for 2.5 minutes, loading continued until the total settlement reached 40 mm (100% of the column diameter).

3.2.2. Results of the single stone column tests

The σ–ε curve shows three characteristic stages: elastic (ε < 1–2%); plastic yielding (ε = 2–4%); failure (ε > 3.5–4%).

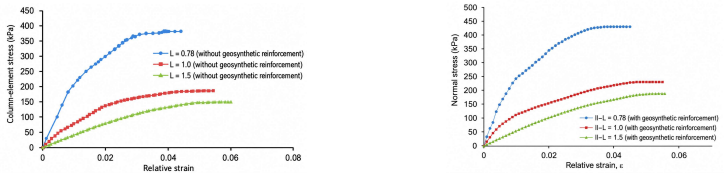

Figure 3.3 Stress–strain relationship of a single stone column in the foundation soil

Key results:

- The ultimate bearing capacity q_{ult} decreases sharply as I_L increases: 378 kPa (I_L = 0.78) → 187 kPa (I_L = 1.0) → 148 kPa (I_L = 1.5), corresponding to decreases of 51.3% and 61.0%.
- The geogrid improves the initial deformation modulus E_i more strongly than σ_{max}: an increase of 45.9% at I_L = 0.78, showing that the geogrid is clearly effective during the elastic stage (ε < 2%).
- The bearing capacity factor $N_c = q_{ult}/c_u$ ranges from 18.7–22.7 at I_L = 0.78 and 1.0 (within the range N_c = 18–25 per FHWA); at I_L = 1.5 it reaches 29.6–37.6, exceeding the recommended range.

Table 3.7 Summary of loading test results for single stone columns

I_L	Geogrid	σ_{max} (kPa)	εmax (%)	E_i (kPa)	Increase in σ_{max} (%)
0.78	No	381.76	3.87%	19962	-
	Yes	429.89	4.50%	29134	12.6
1.0	No	185.90	5.30%	9400	-
	Yes	227.80	5.50%	14000	22.5
1.5	No	149.04	5.90%	4240	
	Yes	186.00	5.60%	5300	24.8

– The dominant failure mode is bulging, at a depth of 2.5D–4D from the column head, consistent with Hughes and Withers (1974) and Law (2015).

3.2.3. Results of the geogrid-reinforced stone column group tests

A 2×2 column group test (D = 40 mm, L = 600 mm) combined with a 200 kN/m geogrid, in clayey silt at I_L = 0.78 with three spacing ratios s/D = 2.5; 3.0; 3.5.

Settlement: Reducing s/D from 3.5 to 2.5 (increasing as from 6.41% to 12.57%): settlement decreased by 52.6% at 120 kPa (from 17.32 mm to 8.21 mm). The settlement rate dS/dp decreased from 0.155 mm/kPa (s/D = 3.5) to 0.070 mm/kPa (s/D = 2.5).

Column-head stress: As s/D increases from 2.5 to 3.5, σ_c at p = 120 kPa increases from 199.02 kPa to 216.05 kPa (an increase of 8.6%) due to less overlap between the zones of influence of adjacent columns.

Foundation soil pressure: At p = 120 kPa, σ_s at s/D = 3.5 (108.07 kPa) is 10% higher than at s/D = 2.5 (98.06 kPa), reflecting the load-distribution efficiency of the arching and membrane effects.

Table 3.8 Settlement survey results of the foundation soil at each load stage in the physical model of the geogrid-reinforced stone column group

s/D	Vertical pressure (kPa)	18	36	54	72	90	108	120
2.5	Foundation soil settlement (mm)	0.845	1.92	2.86	4.136	5.45	6.68	8.21
3.0		1.249	2.65	4.23	6.12	8.11	10.41	12.56
3.5		1.49	3.42	5.8	8.82	11.65	14.48	17.32

Table 3.9 Summary of settlement analysis by spacing ratio s/D for the stone column group

s/D	as (%)	S (mm) at p=120 kPa	Reduction ratio vs. s/D=3.5	Settlement rate vs. load (mm/kPa)	R^2
2.5	12.57	8.21	52.6%	0.070	0.988
3.0	8.73	12.56	27.5%	0.109	0.986
3.5	6.41	17.32	-	0.155	0.992

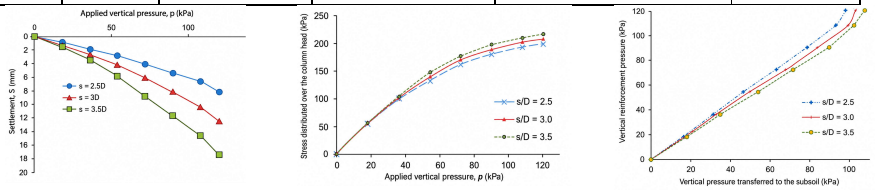

Figure 3.3 Settlement, stress on the stone column heads, and foundation soil pressure under increasing compression load stages

Geogrid strain: The tensile force increases linearly with load and is proportional to the column spacing. At 120 kPa: 3.013 kN/m (s/D = 2.5) increases to 3.670 kN/m (s/D = 3.5), an increase of 21.8%.

Table 3.10 Geogrid strain at each test load stage

Pressure (kPa)	18	36	54	72	90	108	120
s/D= 2.5	0.45	0.89	1.35	1.78	2.25	2.72	3.01
s/D= 3.0	0.52	1.02	1.56	2.06	2.57	3.08	3.44
s/D= 3.5	0.57	1.12	1.67	2.18	2.748	3.31	3.67

3.3. Chapter 3 remarks

Chapter 3 successfully built and operated a 1:20-scale physical model with a total of 18 tests (9 scenarios × 2 repetitions), with a repeat-test error < 5%. The main results are:

- Single stone column: the ultimate bearing capacity q_{ult} ranges from 148–426 kPa depending on the foundation soil state and the presence of the geogrid; the geogrid improves the bearing capacity by 12.7–27.0%, with higher effectiveness in softer soil; the dominant failure mode is bulging at 2.5D–4D.
- Geogrid-reinforced column group: reducing s/D from 3.5 to 2.5 reduces settlement by 52.6%; the settlement rate decreases by 2.2 times; geogrid strain increases by 21.8% as the column spacing increases.
- The results provide a reliable dataset for calibrating the Plaxis 3D numerical model parameters and for proposing calculation formulas in Chapter 4.

CHAPTER 4

BEHAVIOR OF STONE COLUMNS COMBINED WITH GEOGRID REINFORCEMENT IN SOFT SOIL TREATMENT UNDER EMBANKMENT LOADING

Chapter 4 uses the theoretical basis (Chapter 2) and the physical model experimental results (Chapter 3) to analyze the overall behavior of the embankment–stone column–geogrid system using a 3D numerical model in Plaxis 3D, from which formulas are proposed for predicting the ultimate bearing capacity and the stress concentration ratio.

4.1. Behavior of single stone columns combined with geogrid reinforcement from experimental results

4.1.1. Ultimate bearing capacity (q_{ult})

The ultimate bearing capacity decreases sharply as I_L increases: from 378 kPa (I_L = 0.78) to 148 kPa (I_L = 1.5). The geogrid improves the bearing capacity by 12.7% (I_L = 0.78), 21.4% (I_L = 1.0) and 27.0% (I_L = 1.5). The factor $N_c = q_{ult}/c_u$ ranges from 18.7–22.7 at $I_L \leq 1.0$, within the range N_c = 18–25 per FHWA (1983); at I_L = 1.5 it reaches 29.6–37.6 due to a shift in the failure mechanism.

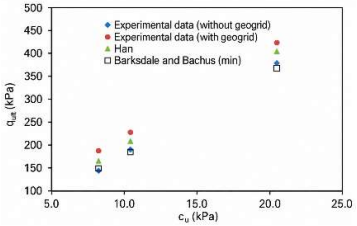

Figure 4.1. Correlation between the ultimate bearing capacity of the stone column (q_{ult}) and the undrained shear strength of the soil c_u

Table 4.1 Calculation results of the ultimate bearing capacity of single stone columns

I_L	c_u (kPa)	E_s (kPa)	q_{ult} (kPa)		Δq (%)	$N_c=q_{ult}/c_u$
			Without geogrid	With geogrid		
0.78	20	1.450	378	426	12.70	18.9–21.3
1.0	10	1.050	187	227	21.39	18.7–22.7
1.5	5	850	148	188	27.03	29.6–37.6

4.1.2. Secant deformation modulus E_{50}

The modulus E_{50} is determined at 50% of the ultimate strength, reflecting the equivalent stiffness under laboratory conditions. The value E_{50} = (4000–25000) kPa

obtained from the research model is significantly lower than the value determined from field tests at the Long Son project ((25000–70000) kPa), due to different foundation soil conditions: the physical model used soft clay (c_u = (5–20) kPa) while Long Son had a stiffer sandy clay (SPT N = 10–11). However, results from both the physical model and the field tests show that E increases as the surrounding foundation soil becomes stiffer. According to Dang et al. (2025), E increases from (25–40) MPa (stage 1) to 70 MPa (stage 2) after ground improvement. With the geogrid present, E_{50} increases by 19% to 27% depending on the foundation soil state.

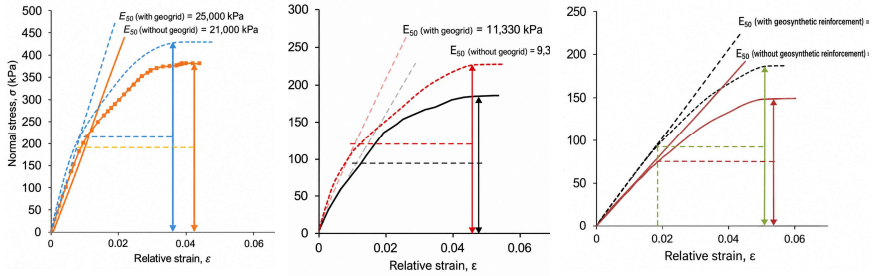

I_L=0.78 I_L=1.0 I_L=1.5

Figure 4.2. Deformation modulus E_{50} of the stone column at 50% of the ultimate load for test cases I_L=0.78; I_L=1.0 and I_L=1.5

4.2. Behavior of geogrid-reinforced stone column groups

The stress concentration ratio n = σ_c/σ_s in the physical model of the column group ranges from 1.83 to 4.56, decreasing as the load increases. At p = 18 kPa, n reaches 3.64 (s/D = 2.5); at p = 120 kPa, n decreases to 1.83–2.03.

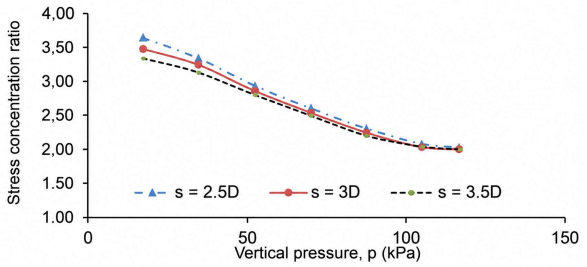

Figure 4.3. Stress concentration ratio from the physical model

The decreasing trend of n reflects the load-distribution mechanism: as the load increases, the surrounding soil gradually takes on more load, resulting in a more balanced load distribution between the column and the soil. The settlement reduction ratio β = Sreinforced / Sunreinforced decreases as the column density increases, consistent with the Priebe (1995) method.

4.3. Construction and calibration of the numerical model

4.3.1. Construction of the numerical model

Geometric factors and boundary conditions

The numerical model is built on the 1/4 unit-cell concept (Balaam and Booker, 1981), exploiting double symmetry. The 1:20-scale physical model was reproduced during the calibration stage: D = 40 mm, s = 100/120/140 mm. Boundary conditions: the base is fully fixed; the lateral boundaries restrain horizontal displacement; the free surface carries a uniformly distributed load of 0–120 kPa.

Mesh generation and sensitivity analysis 15-node wedge elements, Fine configuration with a local refinement factor of 0.5 in the column zone. The difference between the Fine and Very Fine meshes was < 1.5%, while computation time was reduced by 60%.

Table 4.2 Results of the finite-element mesh sensitivity analysis (s/D = 3.0; p = 120 kPa)

Mesh configuration	Number of elements	Column-head settlement (mm)	Deviation from the very-fine configuration (%)	Time (minutes)
Coarse	4 216	8.85	+7.79	4
Fine	9 638	8.32	+1.34	11
Very fine	18 412	8.21	Reference baseline	26

Material model and input parameters

Foundation soil and stone column: the drained Mohr-Coulomb (MC Drained) model. Geogrid: a tension-only geogrid element, EA = 2000 kN/m. Column–soil interface: Rinter = 1.0 (perfect bond) per Law (2015). Main parameters: foundation soil γ = 16.6 kN/m³, c' = 8 kPa, φ' = 20°, E_{50} = 1.20 MPa, ν = 0.33; stone column γ = 18.3 kN/m³, φ' = 38°, ψ = 8°, Ec = 30 MPa, ν = 0.30.

4.3.2. Calibration and verification

A three-step calibration procedure: (1) calibration of the foundation soil without the column; (2) addition of the stone column; (3) verification with the geogrid. Criteria: $R^2 \geq 0.9$, RMSE < 10%. Results: $R^2 > 0.94$ and RMSE < 7% for all cases, confirming that the model reproduces the system's behavior well.

Table 4.3 Calibration and verification results of the numerical model using Plaxis 3D

Comparison quantity	s/D	R^2	RMSE	RMSE (%)	Assessment
Column-head stress σ_c	2.5	0.9892	5.12 kPa	2.57	Satisfactory
Column-head stress σ_c	3.0	0.9415	12.62 kPa	6.09	Satisfactory
Foundation soil pressure σ_s	2.5	0.9828	3.84 kPa	3.92	Satisfactory
Foundation soil pressure σ_s	3.0	0.9966	1.81 kPa	1.76	Satisfactory

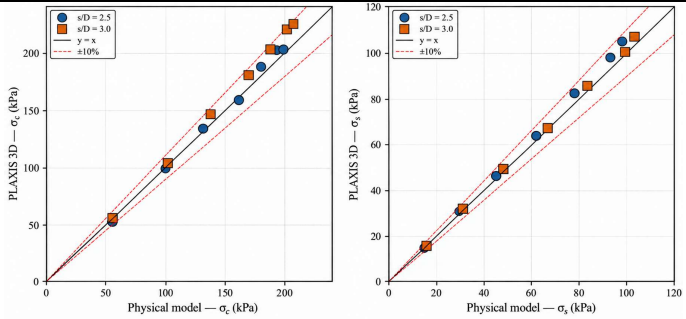

Figure 4.4. Comparison of column-head stress and foundation soil pressure between the physical model and the numerical model

4.4. Factors influencing working efficiency in the numerical model

Four factors were investigated: the column material deformation modulus E_c = (15–55 MPa), the foundation soil deformation modulus E_s = (1–5 MPa), the geogrid stiffness J = (1000–8000 kN/m), and the spacing ratio s/D = (2.5–3.5).

Effect of E_c: The stress concentration ratio n increases as E_c increases. At p = 18 kPa: n increases from 2.72 (E_c = 15 MPa) to 4.56 (E_c = 55 MPa), an increase of 68%. The marginal effect diminishes when E_c > 35 MPa. The range n = 1.83–4.56 falls within the range n = 2.5–5 recommended by FHWA (1983), except for the lowest value recorded at the highest load level.

Effect of E_s: The stress concentration ratio n decreases as E_s increases. At p = 18 kPa: n decreases from 4.87 (E_s = 1 MPa) to 3.13 (E_s = 5 MPa), a decrease of 36%. This is consistent with Ambily and Gandhi (2007).

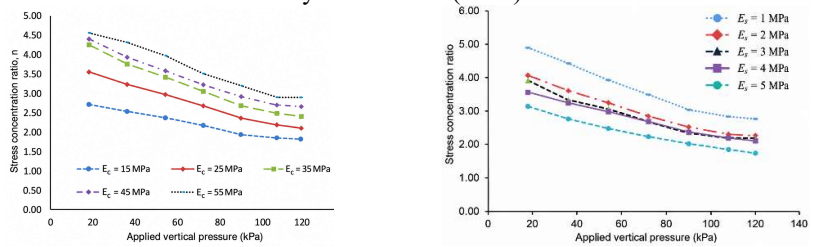

Figure 4.5. Influence of Ec and E_s on the stress concentration ratio

Effect of J: The stress concentration ratio n does not increase linearly with J. J = 3000 kN/m gives the highest n at most load levels. When J is too large, the strain ε decreases, and the membrane effect is not fully mobilized.

Effect of s/D: The stress concentration ratio n increases slightly as s/D increases (difference < 15%). The range s/D = 2.5–3.0 is recommended for design within the scope investigated.

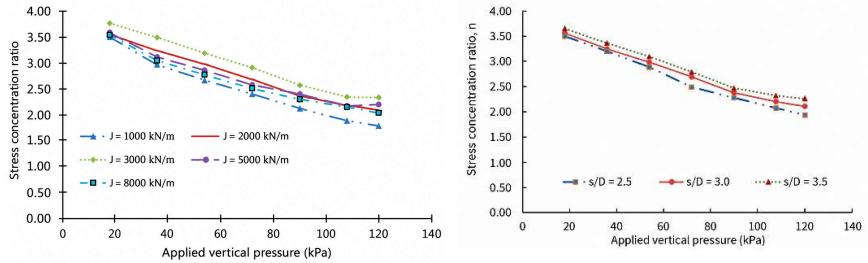

Figure 4.6. Influence of geogrid stiffness and the ratio s/D on the stress concentration ratio

4.5. Proposed calibrated formulas for predicting the bearing capacity and stress concentration ratio of geogrid-reinforced stone column groups

4.5.1. Calibration of the formula for predicting the ultimate bearing capacity

Linear regression $q_{ult} = N_c \cdot c_u$ through the origin, using experimental data at I_L = 0.78 and 1.0:

- Stone column without geogrid: $q_{ult}=18.312 \cdot c_u$ (4-1)
- Stone column with geogrid: $q_{ult}=21.208 \cdot c_u$ (4-2)

Table 4.4 Regression analysis results for the ultimate bearing capacity

Case	N_c	R^2	RMSE (kPa)	Level of improvement
Without geogrid	18.312	0.9997	8.756	Increase of 15.8% (regressed N_c)
With geogrid	21.208	0.9966	10.630	

Theoretical verification: according to the Hughes and Withers (1974) cavity expansion theory with φ_c= 42° (experimental), the theoretical factor $N_c = Kp \cdot [1 + \ln(E_s/(2(1+\nu)\cdot c_u))] \approx 18.31$, nearly matching the regressed factor of 18.312. The increment $\Delta N_c \approx 2.9$ with the geogrid reflects the contribution of the geogrid tensile force to the additional confining pressure.

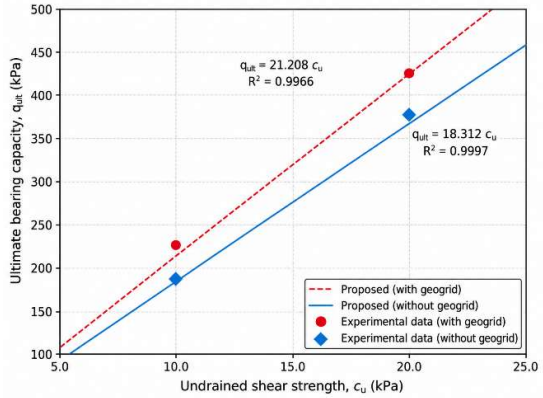

Figure 4.7. Correlation between the ultimate bearing capacity and c_u from regression analysis

4.5.2. Calibration of the formula for the stress concentration ratio

The coefficient n is constructed from two component functions $\sigma_c = f(s/D, p)$ and $\sigma_s = g(s/D, p)$, then taking their ratio: $n = \sigma_c / \sigma_s$ (4-3)

Foundation soil pressure: $\sigma_s = (0.0543*s/D + 0.7458) \cdot p$ (4-4)

with R^2 = 0.996. The coefficient increases as s/D increases, reflecting a greater share of the load carried by the foundation soil at lower column density.

$\sigma_c = A \cdot \ln(p) + B$ (4-5)

$$A = 9\frac{s}{D} + 55{,}82 \text{ and } B = -25{,}03\frac{s}{D} - 112{,}48$$

$$n = \frac{\left(9{,}\frac{s}{D} + 5582\right)\ln p - \left(25{,}03{,}\frac{s}{D} + 11248\right)}{\left(0{,}1{,}\frac{s}{D} + 0594\right)p} \quad (4\text{-}6)$$

The coefficient of determination $R^2 > 0.99$ for all s/D.

Results: R^2 reaches 0.926–0.958 with RMSE < 0.14. The error relative to experimental results decreases from 15–20% (per the current guidance of Han and Ye, 2001) to below 8%. The formula captures the nonlinear variation of n with load p and the influence of s/D.

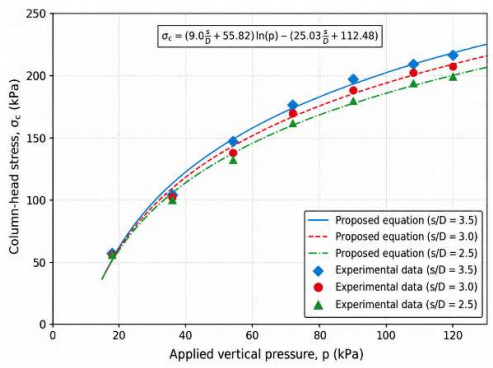

Figure 4.8 Comparison of the column-head stress determined from the physical model test and from the proposed formula

Table 4.5 Coefficient of determination R2 assessing the fit of the proposed formula

s/D ratio	MSE	RMSE	R2
2.5	0.0141	0.119	0.958
3.0	0.0155	0.124	0.947
3.5	0.0178	0.133	0.926

4.6. Application of the calculation to a geogrid-reinforced stone column system for soft soil treatment under actual field conditions

The dissertation applied the proposed formulas to calculate conditions for an actual road project along the Lam River, from Ba Ra bridge to Luu Son bridge, Do Luong district, Nghe An province, section km1+200 – km2+300, and compared the results with FHWA and TCCS 41:2022/TCĐBVN calculations, showing that the proposed formulas give results consistent with field conditions.

Table 4.6 Calculation results of the ultimate bearing capacity q_{ult} of the stone column

c_u (kPa)	Proposed (kPa)	FHWA (min) (kPa)	FHWA (max) (kPa)	Han (2001) (kPa)
12	254.5	216	264	240
15	318.1	270	330	300
20	424.2	360	440	400

4.7. Chapter 4 remarks

- The Plaxis 3D numerical model was successfully built, calibrated and verified, with $R^2 > 0.94$ and RMSE < 7% for all cases.
- The two most important influencing factors are: the column deformation modulus Ec and the foundation soil modulus E_s. The coefficient n = 1.83–4.56; most values (at lower load levels) fall within the range recommended by FHWA, n = 2.5–5, except for the lowest value n = 1.83 (recorded at the highest load level), which is below the lower threshold, reflecting the trend of n decreasing as the load increases. The range s/D = 2.5–3.0 is recommended for design within the scope investigated.
- Proposed calibrated formulas: (1) q_{ult} without geogrid = $18.312 \cdot c_u$; (2) q_{ult} with geogrid = $21.208 \cdot c_u$; (3) $\sigma_s = f(s/D, p)$; (4) $\sigma_c = f(s/D, p)$, from which $n = \sigma c/\sigma s$ is determined
- Scope of application: foundation soil $0.75 \le I_L \le 1.0$ (c_u = 5–25 kPa); stone column D = 0.6–1.0 m, s/D = 2.5–3.5, L/D ≥ 5; geogrid on top of the columns; load p = 18–120 kPa; road embankments and wide-area fills.

CONCLUSIONS AND RECOMMENDATIONS

I. Main conclusions

The dissertation carried out a comprehensive study of the stone-column-geogrid system for soft soil treatment in transportation infrastructure construction, using theoretical research, 1:20-scale physical model testing combined with Plaxis 3D numerical model analysis. The main conclusions are as follows:

1. The working mechanism of the stone-column-geogrid system has been further clarified through the combination of physical and numerical models. The effectiveness of the geogrid depends on the foundation soil state: the improvement in bearing capacity increases from 12.7% (I_L = 0.78) to 27.0% (I_L = 1.5). For soil with $I_L > 1.0$, the low absolute bearing capacity and foundation stiffness reduce the ability to fully mobilize the arching mechanism, so the solution is recommended for application under conditions of $I_L \le 1.0$.
2. The relationship between the spacing ratio s/D and settlement-reduction efficiency has been determined. Reducing s/D from 3.5 to 2.5 (increasing as from 6.41% to 12.57%) reduces settlement by 52.6% at a load of 120 kPa (from 17.32 mm to 8.21 mm). The settlement rate dS/dp decreases from 0.155 mm/kPa to 0.070 mm/kPa, showing that the range s/D = 2.5–3.0 is suitable for practical application within the scope investigated.
3. An important trend was found in the stress concentration ratio (n): the value of n decreases as the load increases, ranging from n = 3.64 (physical model) and 4.56 (numerical model) at 18 kPa down to about n = 1.83–2.03 at 120 kPa. This result provides a basis for refining calculation methods, particularly in estimating the load distribution between the column and the foundation soil at different load levels.
4. A 1:20-scale physical model was successfully carried out with a stone column D = 40 mm, L = 600 mm in soft clay typical of the Red River Delta (Thuong Tin, Hanoi). A total of 9 scenarios × 2 repetitions = 18 tests, with a repeat-test error < 5%.
5. The Plaxis 3D numerical model achieved $R^2 > 0.9$ when verified against the physical model, allowing the parametric study to be extended. The coefficient n = 1.83–4.56; most values fall within the range n = 2.5–5 of Barksdale and Bachus (1983), except for n = 1.83 at the highest load level, which is below the lower threshold of this range; the marginal effect diminishes when Ec > 35 MPa.
6. Comparing calculation methods per FHWA (1983), BS 8006-1:2010, and EBGEO (2011) with the experimental results shows that current methods generally underestimate the improvement in bearing capacity (15–25%) and do not fully account for the influence of the geogrid. Calibrated formulas for predicting q_{ult}, n and β suitable for Vietnamese soft soil conditions have been successfully developed.
7. The bearing capacity of the geogrid-reinforced stone column system increases by 12.7–27.0% compared with a stone column without geogrid, depending on I_L: at I_L

= 0.78, an increase of 12.7% (378 → 426 kPa); at I_L = 1.0, an increase of 21.4% (187 → 227 kPa); at I_L = 1.5, an increase of 27.0% (148 → 188 kPa).

II. New contributions of the dissertation

(1) Development of a systematic experimental dataset on the mechanical behavior (load–settlement–stress distribution–stress concentration ratio) of the stone-column-geogrid system under conditions representative of soft soil in Vietnam, using a 1:20-scale physical model.

(2) Clarification of the influence of the spacing ratio s/D, the physical state of the foundation soil (I_L), and the presence of the geogrid on the stress concentration ratio (n), the settlement reduction ratio (β), and the bearing capacity of the system.

(3) Quantification of the improvement in bearing capacity according to the physical state of the soil (I_L); provision of empirical data supporting the threshold I_L = 1.0 for selecting whether to apply the solution.

(4) Proposal of calibrated formulas for predicting q_{ult} ($R^2 > 0.99$), n ($R^2 > 0.926$) and β for the stone-column-geogrid system, verified against experimental results, numerical model analysis, and existing analytical theory.

III. Limitations

1. The experiments were carried out only on the physical model and the numerical model, without full-scale field-testing conditions. The column-group tests were carried out only at a single value, I_L = 0.78.

2. The study focused on one specific type of soft soil (soft-plastic silty clay, Thuong Tin, Hanoi) with a homogeneous single-layer foundation structure. Multi-layer foundations or other fill materials were not considered.

3. The effect of time on the mechanical properties of the stone column (aging, changes in density) was not considered.

4. Only the case of a column resisting static vertical load was considered; stone columns of varying length, dynamic loading, liquefaction, and slope stability of road embankments were not considered.

5. The numerical model used a simplified Mohr-Coulomb model, without considering more advanced material models or negative pore-water pressure in unsaturated soil.

IV. Recommendations

1. Continue experimental research and field monitoring on a full-scale model, tracking the coefficient n, settlement over time, geogrid tension, and stress distribution with depth.

2. Within the scope of the conditions investigated (c_u = 5–25 kPa, $I_L \leq 1.0$), the research results show that a stone column configuration with s/D = 2.5–3.0 combined with a geogrid of minimum tensile strength 50 kN/m may be considered for application; this configuration gives a settlement reduction of 45–55%, a bearing-capacity increase of 13–27%, and a material saving of 15–20% compared with s/D = 2.0 in the scenarios investigated; further verification is needed when applying it beyond this scope.

3. It is recommended that provisions on the use of geogrid combined with stone columns be added to standards TCCS 41:2022/TCĐBVN and TCCS 66:2015/IBST, including a method for determining the stress concentration ratio accounting for the load level, application conditions based on I_L, geogrid strength requirements, and a construction quality-control procedure.

4. Develop specialized design-support software integrating a Vietnamese soft soil database, the calibrated formulas, and an economic–technical optimization module.

V. Future research directions

1. Study of long-term behavior: the effects of consolidation, degradation of the mechanical properties of the column material, and prediction of residual settlement after 5–10 years in service.

2. Extension of the research to complex geological conditions (multi-layer foundations, organic soil, coastal areas) and special loading conditions (lateral, cyclic, seismic).

3. Comparison of the behavior of end-bearing and floating stone columns, and optimization of column length according to foundation soil properties and design load.

LIST OF PUBLISHED SCIENTIFIC WORKS

1. **Nguyen Hai Ha,** Nguyen Duc Manh, Dang Hong Lam, Nguyen Thai Linh, Vu Bach Tuan. Some factors affecting the behavior of stone columns in soft soil improvement. National Scientific Conference Vietgeo2023 (2023).

(Vietnamese)

2. **Nguyen Hai Ha,** Nguyen Thai Linh. Study on the increase in bearing capacity of crushed-stone columns combined with geotextile on an experimental model. Journal of Transport, No. 9/2023 (733) (2023). (Vietnamese)

3. Pham Thai Binh, Nguyen Duc Manh, **Nguyen Hai Ha**, Le Van Hiep, Nguyen Quang Phuc, Ho Sy An, Nguyen Thai Linh, Indra Prakash, Nguyen Cong Dinh, Nguyen Duc Dam. *Estimation of recompression coefficient of soil using a hybrid ANFIS-PSO machine learning model*. Journal of Engineering Research, Vol.11, Issue 3 (2023).

4. Nguyen Thai Linh, **Nguyen Hai Ha*.** Study on the appropriate selection of the deformation modulus of stone columns in soft soil treatment from experimental results. Journal of Transport, No. 12/2024 (748) (2024). (Vietnamese)

5. **Nguyen Hai Ha,** Nguyen Duc Manh, Nguyen Thai Linh, Le Thi Hong Van. Development of a laboratory experimental model investigating the behavior of stone column groups combined with geogrid in soft soil treatment. National Scientific Conference Vietgeo2025 (2025). (Vietnamese)

6. Nguyen Thai Linh, **Nguyen Hai Ha***, *Nguyen Duc Manh, Indra Prakash, Vu Anh Tuan. Experimental evaluation of a single geogrid-reinforced stone column under varying surrounding soil conditions: Effects on bearing capacity and elastic modulus*. Vietnam Journal of Earth Sciences, 48(2) (2026).

7. Hong Lam Dang, Dinh Cuong Nguyen, **Hai Ha Nguyen**. *A Case Study on the Young's Modulus of Stone Columns Built in Vietnam*. Engineering, Technology and Applied Science Research, Vol. 15, No. 6, 2025, pp. 28629–28634.

8. **Nguyen Hai Ha**, Nguyen Thai Linh, Nguyen Duc Manh, Dang Hong Lam. Study on the settlement reduction ratio of the stone column system for soft soil treatment on an experimental model. Journal of Construction, No. 3/2026. (Vietnamese)

9. **Nguyen Hai Ha**, Nguyen Duc Vinh*. Study on the deformation mechanism of stone columns combined with geogrid using the FLAC 3D numerical model and experiments. Vietnam Bridge and Road Journal, No. 05/2026 (Vietnamese)